15th Triennial World Congress, Barcelona, Spain

APPLICATION OF SENSORLESS ELECTRIC DRIVE TO UNMANNED UNDERSEA VEHICLE PROPULSION

Todd D. Batzel [a], Daniel P. Thivierge [b], and Kwang Y. Lee [c]

[a] *Applied Research Laboratory, State College, PA 16804*
[b] *Naval Undersea Warfare Center, Newport, RI 02841*
[c] *The Pennsylvania State University, University Park, PA 16804*

Abstract: Sensorless electric drive is an enabling technology in the realization of submersible propulsion systems such as the integrated motor/propulsor (IMP). The IMP concept features an electric motor embedded within the shroud of an undersea vehicle's propulsor. This arrangement provides many advantages over conventional propulsion systems but prevents the use of conventional rotor position sensors because of reliability issues in the harsh submerged environment. In this paper, a position sensorless drive is applied to the IMP and experimental results are presented to demonstrate the effectiveness of the proposed technique. *Copyright © 2002 IFAC*

Keywords: Autonomous vehicles, electric vehicles, propulsion control, brushless motors, sensorless drives, motor control, observers, estimation, automatic control

1 INTRODUCTION

Development of an Integrated Motor Propulsor (IMP) for application on an Unmanned Undersea Vehicle (UUV) is underway as part of a joint effort between the Naval Undersea Warfare Center/Newport and the Applied Research Laboratory of the Pennsylvania State University. The IMP concept features an electric motor embedded within the shroud of an undersea vehicle's propulsor. The permanent magnet synchronous motor (PMSM) is the motor of choice for the IMP due to its superior power density, efficiency, and excellent acoustic characteristics.

In order to fully exploit the favorable characteristics of the PMSM, high resolution rotor angle information is required. Typically a resolver or encoder attached to the shaft of the machine provides this information. The structure of the IMP, where the electromagnetics are submerged and installed in the propulsor's shroud, creates difficulty in the use of such position feedback devices. The shaftless IMP system cannot easily accommodate conventional shaft position sensing devices, and the submerged environment poses reliability issues with the use of such sensors. Hall position sensors could be used in close proximity to the submerged magnetics but are undesirable from a reliability and cable routing standpoint. The use of coarse rotor position feedback from Hall effect sensors is also known to generate torque ripple in the PMSM (Jahns, 1984). The integration of the PMSM stator into the UUV propulsor shroud emphasizes the need for torque ripple minimization, since the use of isolation mounts found in conventional shaft driven propulsion systems is not possible.

To address the problems associated with placing a rotor position sensor in the IMP assembly, a *position sensorless* strategy is adopted (Batzel and Lee, 1998, Batzel and Lee, 2000). The hardware implementation for the drive system is described, and experimental results are presented to demonstrate the effectiveness of the proposed controller.

2 IMP CONCEPT

The IMP features an electric motor embedded within the shroud of an undersea vehicle's propulsor. This arrangement eliminates the need for a conventional motor cooling jacket, auxiliary motor cooling system, drive shaft, and shaft coupling. The vehicle interior volume reclaimed by this compact arrangement provides many benefits. The additional payload volume can be used for additional sensors or energy storage to increase mission capability and endurance.

In this concept the electromagnetic stator is installed in the shroud and the permanent magnet rotor is attached to the tip of the hydrodynamic rotor blades. The motor phase leads are routed through the stationary propulsor stator blades to the vehicle hull. The use of conventional fin actuators mounted to the propulsor's shroud is no longer feasible so an engineered elastomer control nozzle has been adopted. The nozzle and associated articulation mechanism are shown schematically in Fig. 1.

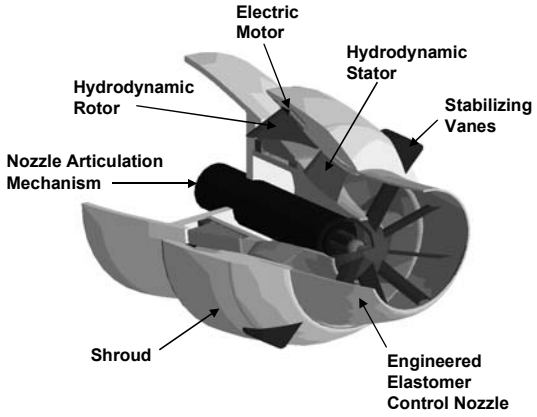

Fig. 1. IMP propulsor configuration.

3 SENSORLESS STRATEGY

The ability to generate smooth torque and perform accurate angular velocity control is of utmost importance toward the success of the proposed IMP concept. These requirements are important from both the vehicle dynamics and control, and radiated noise perspectives. The satisfaction of these requirements without the use of a rotor position sensor requires the adoption of a robust, high fidelity position sensorless strategy. The design and development of such a strategy is presented in the following sections.

3.1 Sensorless PMSM Model

The flux linkage model of the non-salient PMSM in the two-phase stationary reference frame (Batzel and Lee, 2000) is:

$$\frac{d}{dt}\begin{bmatrix}\lambda_\alpha\\ \lambda_\beta\end{bmatrix} = \begin{bmatrix}v_\alpha\\ v_\beta\end{bmatrix} - \tau\left(\begin{bmatrix}\lambda_\alpha\\ \lambda_\beta\end{bmatrix} - \begin{bmatrix}\lambda_{pm\alpha}\\ \lambda_{pm\beta}\end{bmatrix}\right), \quad (1)$$

where

$$\tau = \frac{R}{\frac{3}{2}L_{av}} \quad ; \quad \begin{bmatrix}\lambda_{pm\alpha}\\ \lambda_{pm\beta}\end{bmatrix} = \sqrt{\frac{3}{2}}\lambda_m\begin{bmatrix}\cos\theta\\ \sin\theta\end{bmatrix}. \quad (2)$$

The terms $\lambda_{\alpha,\beta}$ and $v_{\alpha,\beta}$ represent the flux linkages and voltages corresponding to the two fictitious windings – phase α and β. The symbols L_{av}, λ_m, R, and θ represent the self inductance, PM flux constant, resistance, and rotor angle, respectively.

To develop a model for a rotor position observer, the vector $\left[\lambda_{pm\alpha} \;\; \lambda_{pm\beta}\right]^{\mathrm{T}}$ defined in (2) is considered to be a disturbance state that satisfies a known differential equation. Combining the disturbance state vector with the state variables defined in (1) yields the metastate vector, **x**:

$$\mathbf{x} = \left[x_1\; x_2\; x_3\; x_4\right]^{\mathrm{T}} = \left[\lambda_\alpha\; \lambda_\beta\; \lambda_{pm\alpha}\; \lambda_{pm\beta}\right]^{\mathrm{T}}. \quad (3)$$

The input vector is the applied phase voltage in the stationary two-phase reference frame

$$\mathbf{u} = \left[u_1\; u_2\right]^{\mathrm{T}} = \left[v_\alpha\; v_\beta\right]^{\mathrm{T}}, \quad (4)$$

and the output vector, **y**, is chosen to be the measurable currents:

$$\mathbf{y} = \left[y_1\; y_2\right]^{\mathrm{T}} = \left[i_\alpha\; i_\beta\right]^{\mathrm{T}}. \quad (5)$$

Thus, the metasystem state and output equations are described by

$$d\mathbf{x}/dt = A_\omega\mathbf{x} + B\mathbf{u} \quad (6)$$

$$\mathbf{y} = C\mathbf{x}\;, \quad (7)$$

respectively, where

$$A_\omega = \begin{bmatrix}-\tau & 0 & \tau & 0\\ 0 & -\tau & 0 & \tau\\ 0 & 0 & 0 & -\omega_e\\ 0 & 0 & \omega_e & 0\end{bmatrix} \quad ; \quad B = \begin{bmatrix}1 & 0\\ 0 & 1\\ 0 & 0\\ 0 & 0\end{bmatrix} \quad . \quad (8)$$

$$C = \begin{bmatrix}\frac{\tau}{R} & 0 & -\frac{\tau}{R} & 0\\ 0 & \frac{\tau}{R} & 0 & -\frac{\tau}{R}\end{bmatrix}$$

The term ω_e represents the angular velocity of the rotor shaft in electrical radians per second. The subscript ω associated with the A_ω matrix is used to indicate variation with the rotor angular velocity.

Under the assumption that rotor velocity is approximately constant over the system sampling period, the angular velocity may be considered to be a slowly varying PMSM parameter. This assumption is conservative given the large mechanical time

constant of the IMP structure relative to the fast electrical time constant of the motor. With this assumption, the resulting model is a linear time varying system, allowing the use of well-developed linear control methods. It is also stressed that the model given in (6) and (7) does not contain any mechanical variables such as torque, friction, and inertia in the state equations. This is advantageous, since torque and inertia are often unknown and vary during the operation of the system.

3.2 Rotor Position Observer

With angular velocity considered to be a slowly varying parameter, (6) and (7) may be used to construct a full order observer (Luenberger, 1971). The observer is used to estimate the state vector **x** of (3) from knowledge of the input vector **u** and a direct measurement of the output vector **y**. Note that from the estimation of x_3 and x_4, the rotor position estimate $\hat{\theta}$ may be determined from

$$\hat{\theta} = \tan^{-1}\left(\frac{\hat{x}_4}{\hat{x}_3}\right). \tag{9}$$

Using standard observer design techniques for a linear system (Brogan, 1991), the form of the proposed rotor position observer is

$$d/dt\,\mathbf{e} = (A_\omega - GC)\mathbf{e} \tag{10}$$

where **e** is the state estimation error vector

$$\mathbf{e} = \mathbf{x} - \hat{\mathbf{x}}\ , \tag{11}$$

G is the observer gain matrix, and $\hat{\mathbf{x}}$ is the estimated state vector.

The convergence of the estimated state variables toward their actual values is achieved by conventional pole-placement techniques. The eigenvalues of the characteristic equation

$$\left|\lambda I - (A_\omega - GC)\right| = 0 \tag{12}$$

are chosen to have negative real components so that asymptotic state reconstruction is achieved.

Clearly, observability of the system is a requirement for the estimation of PMSM states. The condition for observability is determined by the rank of the observability matrix (Philips and Harbor, 1991):

$$\left[C \;\; CA_\omega \;\; CA_\omega^2 \;\; CA_\omega^3\right]^{\mathrm{T}}. \tag{13}$$

From (13), the system is observable for non-zero angular velocity. This result supports the well-known drawback of the sensorless PMSM – its inability to estimate rotor angle at zero and low angular velocities (Krishnan and Ghosh, 1986; Wu and Slemon, 1992).

Thus, special provisions must be made to start the sensorless PMSM and to operate the system at extremely low angular velocity. For the IMP system, the observer feedback is disabled at speeds below 10 r/s (19 RPM), which represents an experimentally determined low-speed threshold.

3.3 Angular Velocity Estimation

It is clear from (8) that rotor velocity is a required parameter for the implementation of the proposed rotor position observer. In addition, angular velocity feedback is required to accurately track the velocity reference in a speed control loop used in the IMP propulsion system. Therefore, in the absence of an angular velocity sensor, a suitable strategy must be developed to determine this parameter. Two strategies are described in the following sections, and the strengths of each technique are combined to form an adaptive velocity estimation scheme.

Quasi Steady State Velocity Estimation: A quasi steady state estimate for magnitude of the angular velocity (Batzel and Lee, 1998) is

$$\left|\hat{\omega}_e\right| = \frac{\sqrt{(v_\alpha - Ri_\alpha)^2 + (v_\beta - Ri_\beta)^2}}{\sqrt{3/2}\,\lambda_m}. \tag{14}$$

This result suggests the use of the input and output vectors, **u** and **y**, to estimate the magnitude of the angular velocity. The direction of the angular velocity estimate at sampling interval k is then obtained from

$$\hat{\omega}_e = \mathrm{sgn}\big(\phi(k) - \phi(k-1)\big)\left|\hat{\omega}_e\right|, \tag{15}$$

where

$$\phi(k) = \tan^{-1}\left(\frac{Ri_\alpha(k) - v_\alpha(k)}{v_\beta(k) - Ri_\beta(k)}\right). \tag{16}$$

The strength of this method is its ability to determine velocity – even at zero and very low speeds. The weakness is its dependency on PMSM parameters.

Time Derivative of Estimated Rotor Angle: An alternative to the method given in (15) is to use the time derivative of the estimated rotor angle

$$\hat{\omega}_e = d\hat{\theta}/dt\,. \tag{17}$$

This method obviously requires a stable position observer, and the observer pole locations should be much faster than the angular velocity. Both of these constraints may be enforced by proper selection of the system eigenvalues at non-zero angular velocity. Subject to these constraints, the estimated angular velocity obtained by (17) approaches the actual value when averaged over a sufficient period of time.

The drawback to this method is the noise that results from the differentiation process and its inability to obtain an accurate speed estimate at startup, where the rotor position is not observable. The strength of this method is the accuracy of the speed estimates throughout the medium to high speed range.

Adaptive Velocity Estimation: The two proposed velocity estimation methods complement each other nicely. The use of (15) yields good performance at very low speeds, but is subject to parameter uncertainty. The use of (17), however, is essentially independent of the parameter estimation errors so long as the system poles are chosen to be faster than the angular velocity and the velocity is sampled over a sufficient period of time. Thus, the strengths of each method may be combined to form the velocity estimation correction scheme, as shown in Fig. 2.

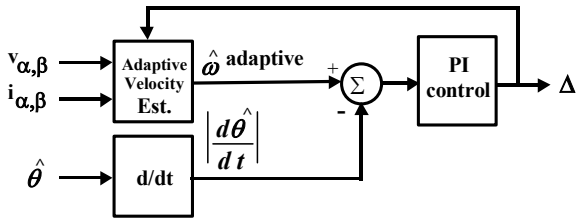

Fig. 2. Velocity estimation correction block.

To use (17) to correct for velocity estimation errors obtained by (15), (14) is modified to include an uncertainty term Δ, which represents the uncertainty in the permanent magnet flux linkage:

$$|\hat{\omega}_e| = \frac{\sqrt{(v_\alpha - Ri_\alpha)^2 + (v_\beta - Ri_\beta)^2}}{\sqrt{3/2}(\lambda_m + \Delta)}. \qquad (18)$$

Initially, the error term Δ is set to zero. However, as long as the magnitude of the estimated velocity is above the low speed threshold where the position observer is assumed to be stable, the adaptive velocity estimation process is activated.

The adaptation process compares the output of (18) with (17) to generate the velocity estimation error. A PI controller operates on the estimation error, adjusting the output Δ to correct for the parameter uncertainty. The time constant of the PI controller is chosen to be slow, since the temperature effect that causes the parameter drift is a very slow effect as well. This has the benefit that the noise generated by the differentiation of the rotor angle estimate is smoothed over time. Thus, as long as the rotor position estimator remains stable, the average value of its derivative is close to the actual rotor speed.

This velocity estimation scheme has been shown through experimentation (Batzel and Thivierge, 2000) to produce accurate tracking of the velocity reference, despite the absence of the position/velocity sensor. This is of critical importance in undersea vehicles where the rotor angular velocity is used to achieve the desired forward vehicle speed.

An overall block diagram of the proposed position observer, including the angular velocity estimation block, is shown in Fig. 3.

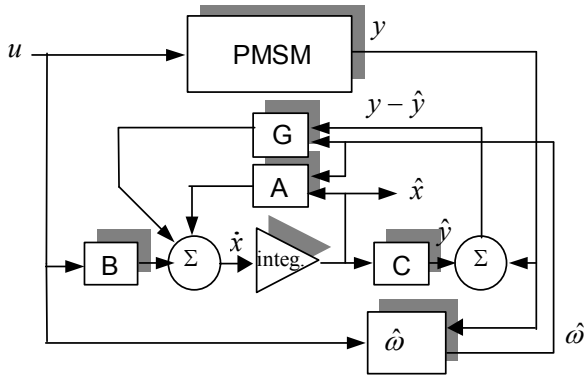

Fig. 3. Block diagram of rotor position estimator.

4 HARDWARE IMPLEMENTATION

The computing hardware for the sensorless electric drive consists of both a Sharc 21061 floating point digital signal processor (DSP), and a fixed point motor control DSP (ADMC401). The floating point DSP performs rotor position and velocity estimation at 100 μs, and 0.5 ms intervals, respectively. The fixed point motor control DSP is used to sample the stator voltages and currents, provide the PWM signals to the inverter, and implement the current control function. The two DSPs communicate directly using a dual-port RAM structure.

The DSP controller board is interfaced to a 3-phase H-bridge power stage consisting of two Powerex 600V, 100Arms six-pack IGBT Intelligent Power Modules (IPMs), and pulse width modulation (PWM) signal isolation and DC/DC converter boards. The IMP motor is a 10 HP permanent magnet synchronous motor manufactured by Magmotor. The motor controller and power stage are shown in Fig. 4, while the IMP motor is shown coupled to an eddy-current dynamometer in Fig. 5.

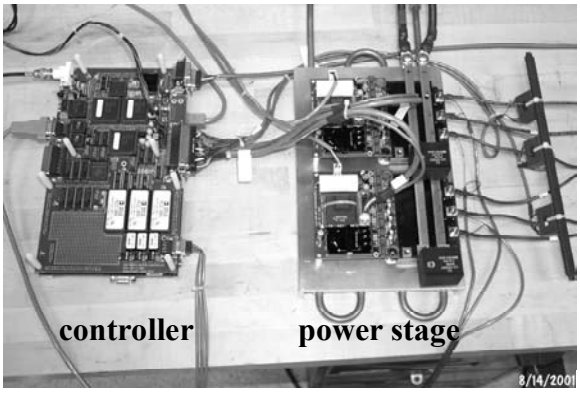

Fig. 4. DSP-based controller and power stage.

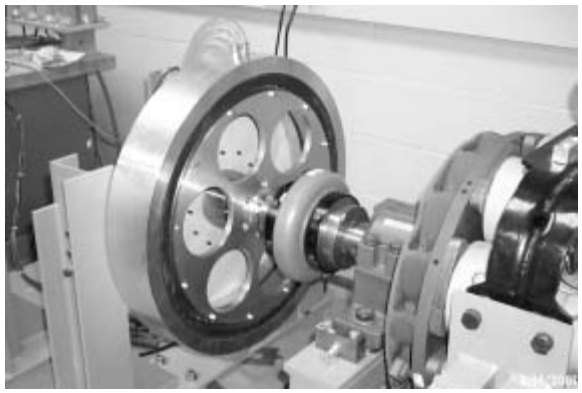

Fig. 5. IMP motor (left) and dynamometer (right).

5 EXPERIMENTAL RESULTS

To evaluate the performance of the prototype sensorless drive, a set of experiments were performed on the IMP where the rotor position observer executes the sensorless algorithm in a real time, closed loop system. The IMP motor parameters are included in Table I, and Fig. 6 shows input, output, and state variable vectors defined in (3)-(5) for operation at 315 RPM and 95 n-m load torque.

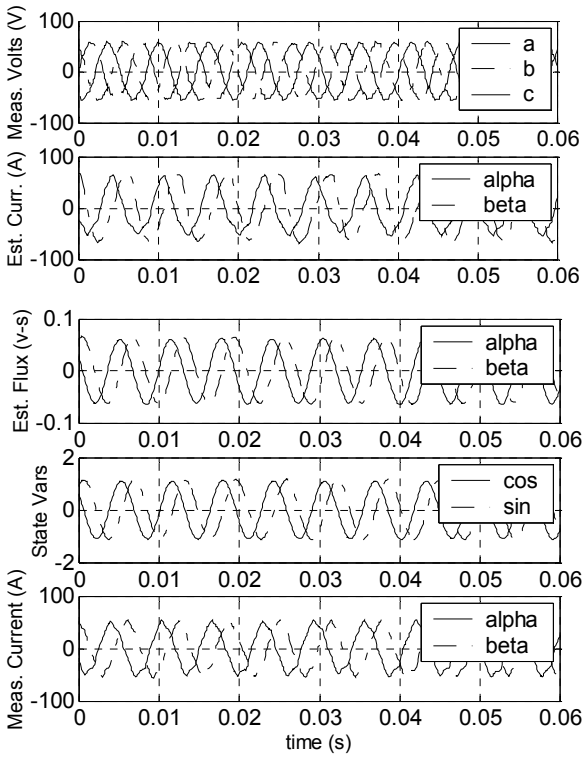

Fig. 6. IMP state estimation at 315 RPM, 95 n-m.

5.1 Rotor Position Estimation Accuracy

In order to evaluate the rotor position estimation accuracy, a resolver was temporarily attached to the hub of the IMP motor. The resolver was used only as a reference for evaluating the accuracy of the estimated rotor position, while the estimated rotor angle was used to commutate the PMSM.

Table I. IMP motor parameters.

Resistance	0.13 Ω
Inductance	0.13 mH
PM Flux Linkage	0.04469 v-s
Rated Power	10 HP
Poles	64

Low speed operation is known to pose difficulties to the sensorless drive due to observer ill conditioning. Fig. 7 shows rotor position estimation accuracy at 23 RPM, which is just above the aforementioned low speed velocity threshold. At this speed, the maximum difference between the resolver position and estimated angle is less than two electrical degrees, an accuracy that is representative of operation across the IMP speed range (<600 RPM).

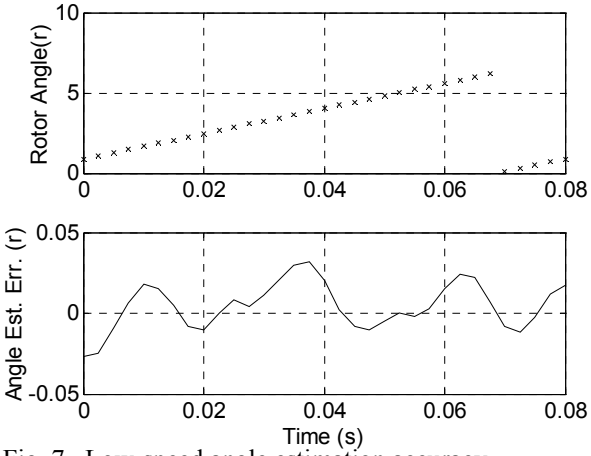

Fig. 7. Low-speed angle estimation accuracy.

5.2 Rotor Position Estimation Robustness

In practical applications, external disturbances such as load torque variations occur regularly, and an effective rotor position estimator must be robust to these events. In this section, robustness to load torque variation is examined.

Because the PMSM model used to construct the rotor position observer does not include mechanical parameters such as friction, inertia, and load torque, the angle estimation accuracy is not expected to be affected by the load torque disturbance. This expectation is confirmed in the experiment shown in Figs. 8 and 9, which depict the angle estimation at an angular velocity of 315 RPM at 13 and 95 n-m load torque, respectively. From these figures, the estimation accuracy is not significantly affected by the load torque, as predicted in previous experiments (Batzel and Thivierge, 2000).

5.3 Sensorless Startup from Zero Speed

The startup of the sensorless IMP is shown in Fig. 10, where an initial angle estimation error of

approximately 11 electrical degrees is present. In this experiment, the initial angle estimate was obtained by forced alignment methods (Matsui and Shigyo, 1992). The figure shows a smooth, dither-free startup despite the velocity estimation polarity reversals at very low speed, where the observer feedback is disabled.

6 CONCLUSIONS

The design of an electric drive system suitable for the Integrated Motor/Propulsor (IMP) has been presented. An enabling technology for the implementation of the IMP is a *position sensorless* electric drive system for the PMSM. The algorithm, and hardware implementation of such a sensorless drive system is set forth in this paper. A series of real-time, closed-loop experiments demonstrate the effectiveness of the proposed sensorless control method over a wide variety of operating conditions. Furthermore, the sensorless system shows robustness to mechanical parameters such as load torque, inertia, and friction.

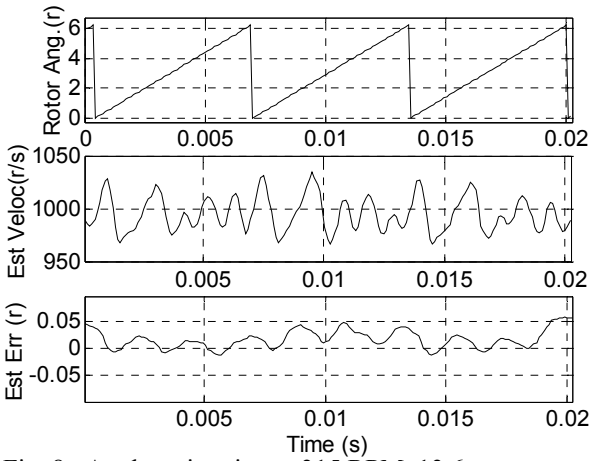

Fig. 8. Angle estimation at 315 RPM, 13.6 n-m.

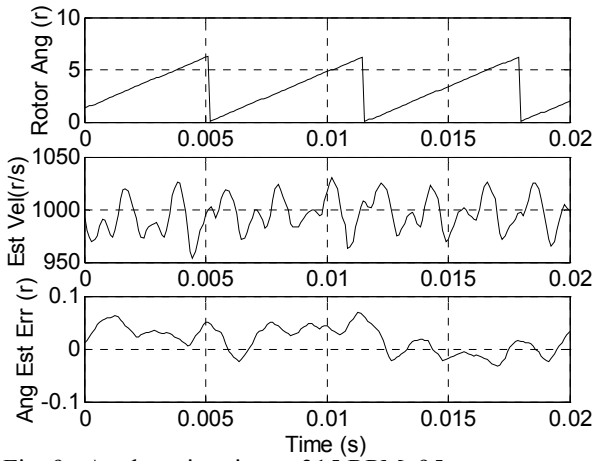

Fig. 9. Angle estimation at 315 RPM, 95 n-m.

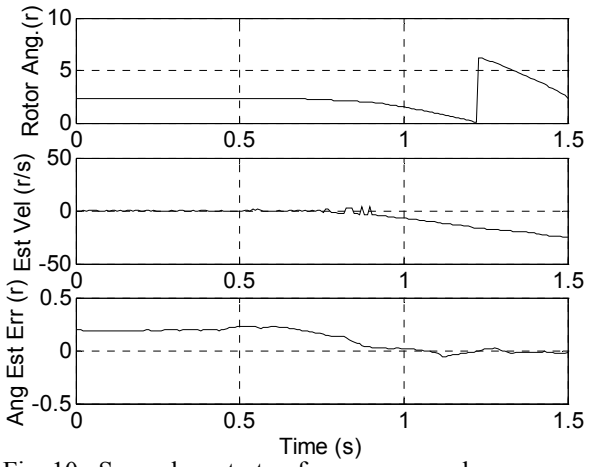

Fig. 10. Sensorless startup from zero speed.

7 ACKNOWLEDGEMENTS

The work outlined in this paper was supported by the Office of Naval Research under Grant N00014-98-1-0718 as well as ONR 333 Underwater Weapons Propulsion and Power Sources program.

8 REFERENCES

Batzel, T.D. and K.Y. Lee (1998). Commutation torque ripple minimization for permanent magnet synchronous motors with Hall effect position feedback. *IEEE Trans. on Energy Conv.*, v. 13, no. 3, pp. 257-262.

Batzel, T.D. and K.Y. Lee (2000). Slotless permanent magnet synchronous motor operation without a high resolution rotor angle sensor. *IEEE Trans. on Energy Conv.*, v. 15, no. 4, pp 366-371.

Batzel, T.D. and D.P. Thivierge (2000). Electric drive for 21" UUV. 3rd *Naval Symposium on Electric Machines* , Philadelphia, PA.

Brogan, W.L. (1991). *Modern Control Theory*, Prentice-Hall, Englewood Cliffs, NJ.

Jahns, T.M. (1984). Torque production in permanent magnet synchronous motor drives with rectangular current excitation. *IEEE Trans. on Industry Applications*, vol. 20, pp. 803-813.

Krishnan, R. and R. Ghosh (1986). Starting algorithm and performance of a PM DC brushless motor drive system with no position sensor. *Power Electronic Specialists Conference*, pp. 815-821.

Luenberger, D. (1971). An introduction to observers. *IEEE Trans. on Automatic Control*, vol. AC-16, no. 6, pp. 596-602.

Matsui, N. and M. Shigyo (1992). Brushless DC motor control without position and speed sensors. *IEEE Trans. on Ind. Apps.*, vol. 28, no. 1, pp. 120-127.

Phillips, C. and R. Harbor (1991). *Feedback Control Systems*, Prentice Hall, Englewood Cliffs, NJ.

Wu, R. and G. Slemon (1991). A permanent magnet motor drive without a shaft sensor. *IEEE Trans. on Ind. Apps.*, vol. 27, no. 5, pp. 1005-1011.